

Rafting in single crystal nickel-base superalloys – An overview

M KAMARAJ

Department of Metallurgical Engineering, Indian Institute of Technology –
Madras, Chennai 600 036, India
e-mail: kamaraj@iitm.ac.in

Abstract. Currently nickel-base single crystal (SX) superalloys are considered for the manufacture of critical components such as turbine blades, vanes etc., for aircraft engines as well as land-based power generation applications. Microstructure and high temperature mechanical properties are the major factors controlling the performance of SX superalloys. Rafting is an important phenomenon in these alloys which occurs during high temperature creep. It is essential to understand the rafting mechanism, and its characteristics on high temperature properties before considering the advanced applications. In this review article, the thermodynamic driving force for rafting with and without stress is explained. The nature and influence of rafting on creep properties including pre-rafter conditions are discussed. In addition, the effect of stress state on γ/γ' rafting, kinetics and morphological evolution are discussed with the recent experimental results.

Keywords. Single crystal superalloys; rafting; multiaxial stress states; creep; kinetics of rafting; parabolic growth of γ -channel width.

1. Introduction

Single crystal (SX) superalloys are a group of nickel-base superalloys. They exhibit superior high temperature mechanical strength (at temperatures as great as 85% of their melting points) and hot corrosion resistance compared to conventional superalloys. Owing to these attractive properties, SX superalloys are candidate materials for high temperature critical components such as gas turbine blades and vanes in modern aircraft engines, aero-space and power generating plants (Sims & Hagel 1972; Sahm & Speidel 1974; Meetham 1981; McLean 1983). The high temperature mechanical properties of SX superalloys are strongly derived from: (i) design of chemical compositions, and (ii) their microstructure. The chemical compositions of several SX alloys are listed in table 1. The microstructure of SX alloys consists of a high volume fraction (about 70 volume percent) of γ' coherently precipitated in a face centred cubic (*fcc*) γ matrix (see figure 1). The volume fraction and morphology of γ/γ' phases are controlled and optimized by a standard stepwise heat treatment in order to obtain a specific set of high temperature mechanical (creep, fatigue and thermal fatigue) properties.

During service, SX components must be able to withstand, at high temperatures, gases emerging from the combustion chamber and experience a combination of high temperature

Table 1. Chemical composition (wt.%) of single crystal superalloys.

Alloy	Element												Density (kg/cm ³)
	Cr	Co	Mo	W	Ta	Re	V	Nb	Al	Ti	Hf	Ni	
<i>First generation</i>													
PWA 1480	10	5	-	4	12	-	-	-	5	1.5	-	Bal.*	8.7
PWA 1483	12.8	9	1.9	3.8	4	-	-	-	3.6	4	-	Bal.	-
Rene N4	9	8	2	6	4	-	-	0.5	3.7	4.2	-	Bal.	8.56
SRR 99	8	5	-	10	3	-	-	-	5.5	2.2	-	Bal.	8.56
RR 2000	10	15	3	-	-	-	1	-	0.05	4	-	Bal.	7.87
AM1	8	6	2	6	9	-	-	-	0.05	1.2	-	Bal.	8.59
AM3	8	6	2	5	4	-	-	-	5.2	2	-	Bal.	8.25
CMSX-2	8	5	0.6	8	6	-	-	-	6	1	-	Bal.	8.56
CMSX-4	8	5	0.6	8	6	-	-	-	5.6	1	-	Bal.	8.56
CMSX-6	10	5	3	-	2	-	-	-	4.8	4.7	0.1	Bal.	7.98
CMSX-11B	12.5	7	0.5	5	5	-	-	0.1	3.6	4.2	0.1	Bal.	8.44
CMSX-11C	14.9	3	0.4	4.5	5	-	-	0.1	3.4	4.2	0.04	Bal.	8.36
SX 792	12	8	2	4	5	-	-	-	3.4	4.2	0.04	Bal.	8.25
SC 16	16	-	3	-	3.5	-	-	-	3.5	3.5	-	Bal.	8.21
<i>Second generation</i>													
CMSX-4	6.5	9	0.6	6	6.5	3	-	-	5.6	1	0.1	Bal.	8.7
PWA 1484	5	10	2	6	9	3	-	-	5.6	-	0.1	Bal.	8.95
SC 180	5	10	2	5	8.5	3	-	-	5.2	1	0.1	Bal.	8.84
MC2	8	5	2	8	6	-	-	-	5	1.5	-	Bal.	8.63
Rene N5	7	8	2	5	7	3	-	-	6.2	-	0.2	Bal.	NA
<i>Third generation</i>													
CMSX-10	2	3	0.4	5	8	6	-	0.1	5.7	0.2	0.03	Bal.	9.05
Rene N6	4.2	12.5	1.4	6	7.2	5	-	-	5.75	-	0.15	Bal.	8.98

*Balance

(exceeding 1000–1100° C) and stresses (centrifugal and bending forces). Under the combined influence of stress and temperature, initial γ' -cuboidal particles transform into plates

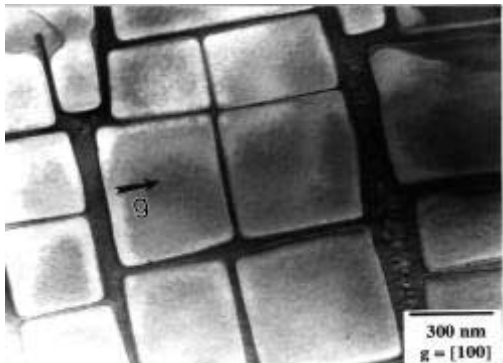
**Figure 1.** Typical micrograph of Ni-base superalloy single crystal (CMSX-4).



Figure 2. SEM micrograph showing rafting in SX superalloy.

which are usually called rafting (see figure 2). This microstructure is also referred to as directional coarsening/lamellar structure (Tien & Copley 1971; Tien & Gamble 1972; Carry & Strudel 1978; MacKay & Maier 1982; Nathal *et al* 1982; Caron & Khan 1983). Rafting was considered as a hardening process which enhances the creep behaviour of SX alloys in the (001) orientation. When the lamellar structure forms perpendicular to the stress, the movement of dislocation by climb over the γ' particle would be eliminated (Pearson *et al* 1980, 1981). Further creep deformation could occur only by the more difficult process of shearing of the γ' phase. Thus the resistance to deformation could increase. Some recent experimental studies have shown opposite effects and demonstrated that the directional coarsening is a softening process which deteriorates high temperature mechanical properties (Henderson & Mclean 1983; MacKay & Ebert 1983; Pollock & Argon 1992; Mughrabi *et al* 1994). Therefore it is important to understand the high temperature characteristics of γ/γ' phases and their kinetics on creep resistance of single crystal superalloys. The purpose of this paper is to review critically the rafting phenomena in SX superalloys and the effects of rafting on deformation behaviour based on our experimental results and other recent studies from the literature.

2. Driving force for rafting

It is well known that the phenomenon of rafting occurs when single crystal superalloys are subjected to stress at elevated temperature ($T > 900^\circ \text{C}$). It is evident from numerous experimental and theoretical investigations that rafting/directional coarsening is strongly controlled by the sign of applied stress, lattice misfits (d) and elastic constants between γ/γ' phases (Pineau 1976; Chang & Allen 1991; Svetlov *et al* 1992; Ignat *et al* 1993; Socrate & Parks 1993; Pollock & Argon 1994; Nabarro 1996, 1997; Nabarro *et al* 1996; Svoboda & Lukaš 1996; Véron *et al* 1996; Fährmann *et al* 1996; Laberge *et al* 1997; Mukherji *et al* 1997; Ohashi 1997; Paris *et al* 1997; Henderson *et al* 1999).

Most of the single crystal superalloys have negative lattice misfit (i.e. where the lattice constant of the ordered $a\gamma'$ phase is smaller than the lattice constant of the $a\gamma$ phase) which is defined as $\delta = 2(a\gamma' - a\gamma)/(a\gamma' + a\gamma)$. The magnitude of δ is ≈ -0.001 at room temperature and varies with service temperature due to the different thermal expansion coefficients of γ/γ' phases. To explain rafting phenomenon, a typical γ/γ' structure with negative misfit is considered. Figures 3a and b show internal stresses in the absence and in the presence of an external stress respectively. Figure 3a suggests that for $\sigma_{\text{ext}} = \text{zero}$, the chemical potentials of the phases at points 1 and 2 (γ' -particle in the lower right of figure 3a) are equal and

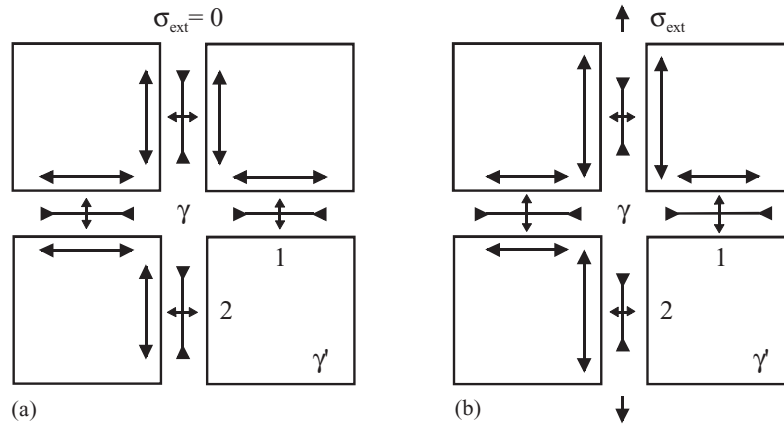


Figure 3. Schematic illustration of internal stress components in a γ/γ' -microstructure. $\sigma_{\text{ext}} = 0$ (a) and > 0 (b) (note that the external stress modifies the internal components) (Kamaraj 1998).

normal non-directional coarsening is expected. In figure 3b an external stress is applied and the situation is characterised by stress components which, unlike in figure 3a, are not equal at positions 1 and 2. The major effect of the external applied stress in figure 3b is that the local stresses are modified in the direction of the applied stress. In the direction perpendicular to the external stress axis in figure 3b stresses change due to the different Poisson numbers of γ and γ' ; however, but this effect is small. All stress components combine to yield one specific value for the hydrostatic stress σ_H ($\sigma_H = \frac{1}{3}(\sigma_1 + \sigma_2 + \sigma_3)$) which is known to directly influence the chemical potential of atoms, (Kamaraj 1998). Tensile stresses act in the γ' -particles parallel to the γ -channels. These are balanced by compressive stresses in the γ -channels parallel to the γ' -surfaces which are much larger than small tensile stress components which act perpendicular to the channels.

Normal non-directional γ' -coarsening at high temperatures is driven by the tendency to decrease the overall γ/γ' -interface energy of the system. Therefore σ_H and, thus the chemical potential of atoms which is directly influenced by σ_H (Swalin 1967), are different. Differences in chemical potential of atoms are known to act as driving forces for diffusion (Shewmon 1989). In summary, the chemical potentials of atoms at positions 1 and 2 which were equal in the absence of an external stress (see figure 3a) are no longer equal when an external stress is applied (see figure 3b). This results in a driving force for diffusion and finally produces the effect of rafting which has been described in the literature in great detail (Swalin 1967; Tien & Copley 1971; Pineau 1976; Nathal *et al* 1982; Shewmon 1989; Henderson & Mclean 1983; MacKay & Ebert 1983; Chang & Allen 1991; Pollock & Argon 1992; Svetlov *et al* 1992; Laberge *et al* 1997; Ohashi *et al* 1997; Paris *et al* 1997; Nabarro 1997; Chen & Immarrigeon 1998; Kamaraj *et al* 1998; Henderson *et al* 1999). Classical treatments (Tien & Copley 1971; Nathal *et al* 1982; Paris *et al* 1997) as well as recent reviews describe the mechanisms and models of directional coarsening or rafting in single crystal superalloys.

3. Effect on creep properties

Compared to conventional superalloys, single crystal (SX) superalloys show a significant increase in creep strength/temperature capability. It is widely accepted that the improvement

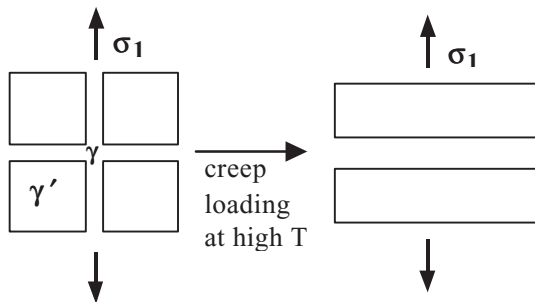


Figure 4. Rafting of a negative misfit alloy: loaded in $\langle 100 \rangle$ -tension creep.

of these alloys is based on their microstructures containing 68–70 vol.% of fine, coherent γ' (with an average size of $0.45\mu\text{m}$) phase. In service, these SX alloys are subjected to uniaxial tension due to high operational centrifugal forces and so most of the investigations are devoted to study the microstructural and mechanical aspects of single crystal superalloys under uniaxial test conditions. A microstructural analysis of the creep process based on metallographic observations (Leverant & Kear 1970; Tien & Copley 1971; Nathal & Ebert 1985; Nathal 1987; Nathal & Mackay 1987; Nathal *et al* 1989; Feller-Kniepmeier & Link 1989; Schneider *et al* 1992; Schneider & Mughrabi 1993) suggests that the creep characteristics are controlled by the three interconnected microstructural processes: (i) the increase of dislocation density in the γ -channels (dislocation glide & dislocation climb) which controls primary creep, (ii) pair wise cutting of two dislocations from a γ -channel into the γ' -phase followed by their annihilation and (iii) the coarsening of γ -channels associated with rafting in later stages of creep which can result in a low but steady increase of creep rate in tertiary creep. Numerous studies have demonstrated that depending on the sign of lattice misfit, two types of directional coarsening of γ/γ' phases formed during prolonged period of time in application of stress and temperatures in $\langle 001 \rangle$ oriented nickel-base single crystal alloys: Type *N* (normal): the cuboids coarsen preferentially transverse to the direction of the externally applied stress and Type *P* (parallel): the cuboids coarsen preferentially parallel to the direction of the externally applied stress. Figure 4 illustrates the raft formation in the negative misfit alloy with the orientation of $\langle 001 \rangle$ under tensile stress and raft forms perpendicular to the axis of the applied stress σ_1 .

In the literature, large volume experimental data is available on the creep behaviour of the single crystal (SX) superalloys (Leverant & Kear 1970; Tien & Copley 1971; Nathal & Ebert 1985; Nathal 1987; Nathal & Mackay 1987; Nathal *et al* 1989; Feller-Kniepmeier & Link 1989; Schneider *et al* 1992; Schneider & Mughrabi 1993; Mughrabi *et al* 1995, 1997; Royer *et al* 1995; Lukas *et al* 1996; Mayr *et al* 1996; Dlouhy & Eggeler 1996; Dlouhy *et al* 1997; Eggeler & Dlouhy 1997). However, the influence of rafting on the creep properties of SX superalloys is not well understood. For example, Pearson *et al* (1980, 1981) and Mackey & Ebert (1983) reported that the coarsening of γ' -phase in SX alloys increases the creep resistance during creep; the rafted morphology suppresses dislocation bypass mechanism and consequently the γ' -shearing may operate which is the slowest recovery process resulting in improved creep resistance. Kondo *et al* (1996) made an attempt to show the effect of pre-rafting of γ' -phase on creep behaviour of the CMSX-4 superalloy. It was found that the radius of dislocation curvature increases with increasing γ -channel thickness in prior creep-tested specimens, resulting in the decrease of applied shear stress and the increase in creep rate. It was concluded that the creep resistance of the alloy depends on the radius of dislocation curvature which is based on the γ -thickness.

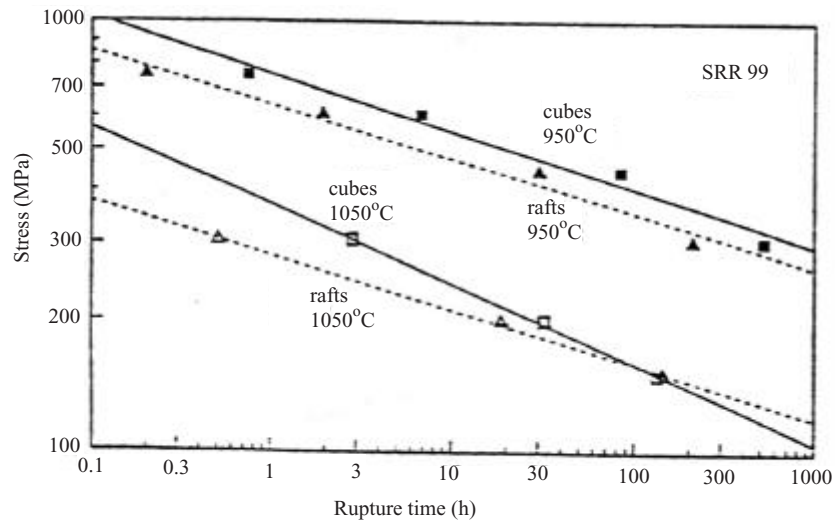


Figure 5. Comparison of creep properties of the as-received and pre-rafted monocrystalline superalloy (Mughrabi 1996).

Recently, Mughrabi (1996) has shown the effect rafting on creep properties of the SRR99 SX superalloy. Figure 5 shows stress rupture diagram for SRR99 in different tested conditions. It is interesting to note that the creep data obtained on the two types of specimens at 950° C show that at all stress levels investigated the specimens with the cuboidal γ' -particles exhibited longer creep lives than those of pre-rafted specimens. However, at 1050° C the pre-rafted specimens tested at high stress level exhibit smaller creep lives but the situation changes the stress level below 150 MPa, pre-rafting improves the creep strength under a given temperature and stress. These experimental data clearly indicate that two recovery creep mechanisms may be operative depending on the test/service conditions namely: (i) low temperature (temp, < 950° C) and high stress (LTHS) and (ii) high temperature and low stress (HTLS). In the case of LTHS, the initial cuboids are not altered and the strain rate is largely dependent on the movement of the dislocations in the combined displacement of glide and climb process at the γ/γ' -interfaces. When the relative escape rate of interfacial dislocations is reduced and the internal stress is large enough to cut the γ' -plates, the dislocation path is reduced and a larger creep rate would be anticipated. But in the case of HTLS, the initial γ' -particles are transformed to lamellar structure, the interfacial dislocations circumvent the rafts (without cutting γ' -particles) which increases the dislocations path resulting the rafted material exhibiting longer creep life.

4. Influence of stress state on rafting

During service, the SX alloys components are not only subjected to uniaxial tension but also to biaxial state of stress in some regions. These stresses are generated due to (i) the thermal gradients in cooled regions, (ii) bending stresses exerted by the flowing gas on the blade and (iii) local stress concentrations. In these circumstances, rafting in real components occurs under a multiaxial state of stress and, it is therefore, important to study how multiaxial stress states influence this process. Eggeler and co-workers proposed a new

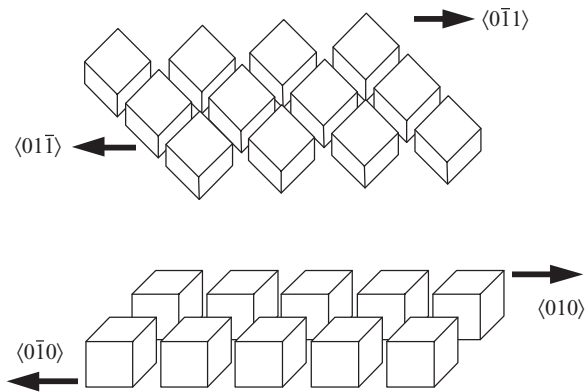


Figure 6. Schematic illustration of the spatial arrangement of γ' -particles during shear testing in the two MCSSs.

shear test technique which was used to study the influence of stress state on γ/γ' - rafting (Mayr 1994; Mayr *et al* 1995, 1996; Dlouhy & Eggeler 1996; Dlouhy *et al* 1997; Eggeler & Dlouhy 1997; Peter *et al* 1997; Kolbe *et al* 1998; Srinivasan *et al* 2000). A few studies have been carried out to understand the rafting characteristics under multiaxial stress conditions (Ignat *et al* 1993; Kamaraj *et al* 1998). In a recent work of our research group (Kamaraj *et al* 1998) the influence of biaxial stress state on rafting in the CMSX-6 single crystal superalloy is discussed. Double shear creep specimens as described earlier (Mayr 1994; Mayr *et al* 1995) were used to obtain two macroscopic crystallographic slip systems (MCSSs): $\{011\}\langle 01\bar{1} \rangle$ and $\{100\}\langle 010 \rangle$. A schematic drawing of the γ' -morphology in these two macroscopic crystallographic slip systems (MCSSs) during shear deformation is given in figure 6.

Shear creep tests were performed at 1025° C in air at a stress level of 85 MPa up to a total strain of 0.048 and 0.062 for the shear systems $\{011\}\langle 01\bar{1} \rangle$ and $\{100\}\langle 010 \rangle$ respectively. Figure 7a shows the arrangement of loading on the specimen and the examination of the

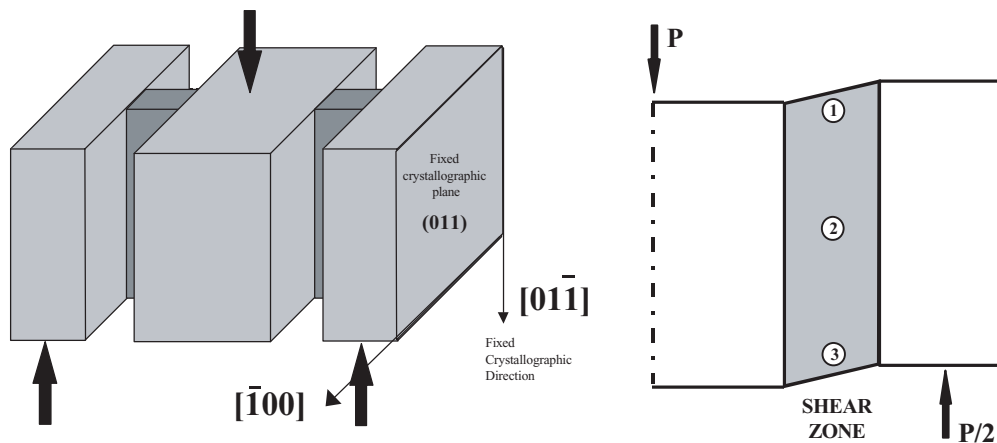


Figure 7. (a) Double shear creep specimen configuration, and (b) locations examined γ/γ' phases in the shear zone. The figure only shows the right half of the specimen in (a) (P: shear load) (Kamaraj *et al* 1998).

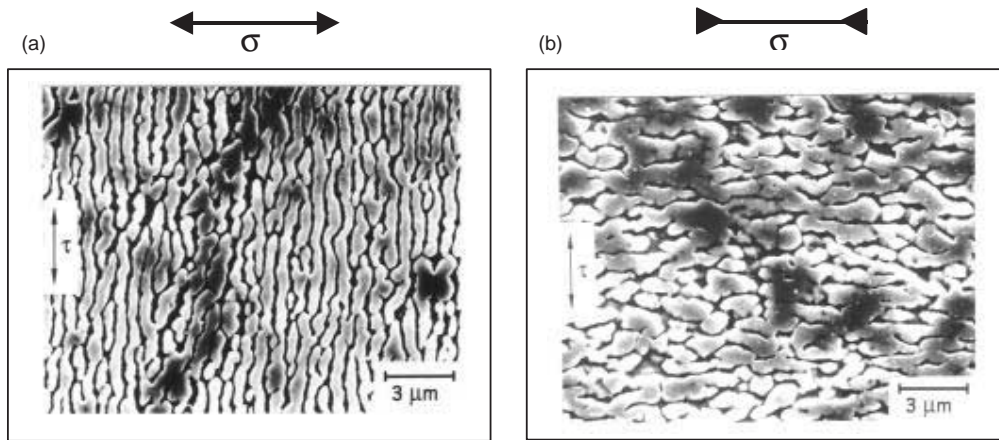


Figure 8. SEM micrographs showing the rafting characteristics of γ/γ' phases after double shear creep. $\{100\}\langle 010\rangle$, $\tau = 85$ MPa ($|\sigma| \geq |\tau|$), position 3 **(a)** and position 1 **(b)**.

microstructure in the shear zone respectively. After testing, the specimens were investigated at three locations in the shear zone denoted 1, 2, and 3 as shown in figure 7b.

It has been shown (Peter *et al* 1997) that the stress state at position 2 is pure shear. In contrast, there are bending stresses at positions 1 (compression) and 3 (tension) which act perpendicular to the direction of the applied load (Peter *et al* 1997). The corresponding FEM - results are reported (Peter *et al* 1997). The specimens were prepared by standard metallographic techniques and examined by means of scanning electron microscopy (SEM). Figure 8 shows the raft morphologies which were obtained for the MCSS $\{100\}\langle 010\rangle$ at position 3 (figure 8a) and position 1 (figure 8b).

The direction and sign of bending stresses s are denoted in figure 8a (shear system: $\{100\}\langle 010\rangle$) and figure 8b (shear system: $\{100\}\langle 010\rangle$); and for the MCSS $\{011\}\langle 01\bar{1}\rangle$ at position 2 (see figure 9a), the bending stress at position 2 is zero, figure 9a (shear system:

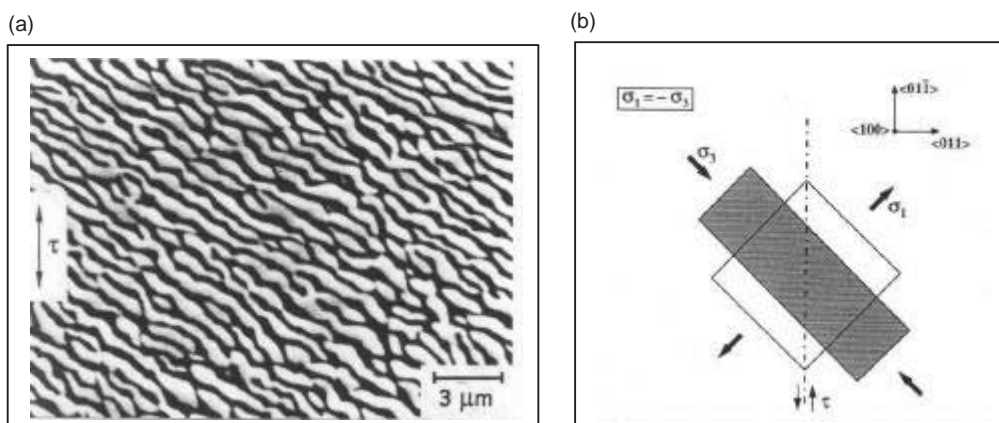


Figure 9. Raft morphology **(a)** and schematic diagram **(b)** of raft formation of γ' -particles in the MCSS $\{011\}\langle 01\bar{1}\rangle$.

$\{011\}\langle 01\bar{1}\rangle$). It can be seen that rafting occurs parallel to the shear direction at position 3 (see figure 8a) and perpendicular to the shear direction at position 1 (see figure 8b). This represents a microstructural proof for the FEM (Mayr 1994; Peter *et al* 1997) which shows that there are significant bending stresses at the outer limits of the shear zones. Thus the γ' -particles of the MCSS $\{100\}\langle 010\rangle$ behave as expected in that they grow perpendicular to a tensile stress component (see figure 8a) and parallel to compressive stress components (see figure 8b). The results on rafting at positions 1 and 3 are in agreement with the work of Ignat *et al* (1993) where this type of rafting was observed in a four point bending creep test.

No directional coarsening in the MCSS $\{100\}\langle 010\rangle$ was observed at position 2 where the stress state is pure shear. In the case of the MCSS $\{011\}\langle 01\bar{1}\rangle$ rafting occurs in an angle of 45° to the direction of the applied stress as shown in figure 9a. This can be rationalised by decomposing the shear stress τ in its maximum principal stresses σ_1 and σ_3 (see figure 9b). In figure 9 (a), γ' -particle is seen to react as we would expect: it coarsens perpendicular to σ_1 and parallel to σ_3 . The present study shows that rafting of γ' -particles during high temperature low stress creep of single crystal superalloy depends on the stress state. There are cases where local bending stress in a shear specimen can be detected (MCSS $\{100\}\langle 010\rangle$). In other cases MCSS $\{011\}\langle 01\bar{1}\rangle$ the presence of biaxial stress state ($\sigma_1 = -\sigma_3$) was found to result in γ' -rafting in an angle of 45° to the direction of the shear stress. Thus it has been clearly demonstrated that γ' -rafting can be used as an indicator for stress states in SX components.

Moreover it is also important to quantitatively evaluate the kinetics of the coarsening of γ' -particles under multiaxial creep conditions. These preliminary results underline need to study the effect of biaxial stress states on rafting in other MCSSs. Recent work of Biermann *et al* (2000) explained the influence of shot peening (which produces biaxial compressive stress state) on the γ/γ' -microstructure. It was concluded that the development of rafting in the shot peened samples, before and after aged ($T = 1050^\circ\text{C}$, $t = 24\text{h}$), is due to internal microstresses modified by plastic deformation and not by the residual macrostress state induced by shot peening (Biermann *et al* 2000).

5. Influence of stress state on the kinetics of γ -channel widening

Under high temperature creep conditions, the occurrence of rafting in single crystal superalloys is basically due to stress-assisted diffusion controlled process and the kinetics of rafting is dependent on the test temperature and time. Veron *et al* (1996) described the role of plasticity on rafting and the expected preferential directional geometry of rafting in P-type and N-type misfit superalloys using morphology maps. Fahrman *et al* (1996) studied the effect of pre-strain and the development of rafting during ageing. It was concluded that the pre-strain paths modify the initial structure γ/γ' interfaces and the local state of stress contributes the driving force for rafting. Recently Matean *et al* (1999) made an attempt to study the coarsening kinetics on CMSX-4. The experimental results revealed that the rafting kinetics alters in elastic as well as plastic regime. Further, it was pointed out in the plastic regime, loss of coherency and reduction in elastic misfit strains are responsible for providing the kinetic path which enables raft development at a reasonable speed.

Recent work by our group (Kamaraj *et al* 2000) compared the kinetics of rafting in CMSX-4 in $\langle 001\rangle$ tension and in $\{011\}\langle 01\bar{1}\rangle$ shear creep testing at a constant maximum

principal stress $\sigma_1 = 50$ MPa at 1080° C for different time intervals. Details of the technique and quantitative evaluation of channel widths are published elsewhere by Kamaraj *et al* (2000). The widening of the γ -channels is characterised by a parabolic rate law and is given by

$$\Delta W = C_1 \cdot (t)^{1/2}, \quad (1)$$

where Δw is the increase in channel width, C_1 is a material and temperature dependent constant and t is time. In order to determine the parabolic rate constant from 1, Δw is obtained from the measurement of an average channel width $w(t)$ at a given time t as

$$\Delta w = w(t) - w_0 - \Delta w_{MC}, \quad (2)$$

where $W(t)$ is the average channel width at a given time, W_0 average initial channel width, Δw_{MC} is the change of channel width due to change of γ/γ' morphology. Δw is then plotted as a function of $(t)^{1/2}$; C_1 is then obtained from a least square fit to the $\Delta w/(t)^{1/2}$ -data. The change in γ' -morphology (from cubes to plates) results in an increase of width of the γ -channels perpendicular to σ , which we refer to as Δw_{MC} (MC for ‘‘morphology change’’):

$$\Delta w_{MC} = 2 \cdot (2 \cdot w_0 \cdot s_0^2 + w_0^2 \cdot \dots \cdot s_0) / [2 \cdot (w_0 + s_0)^2] \quad (3)$$

s_0 and w_0 are the initial average γ' -cube edge length and the initial γ -channel width respectively. figure 10 shows the morphological change γ/γ' phases in both $\langle 100 \rangle$ -tensile and $\{011\}\langle 01-1 \rangle$ -shear creep testing.

It is interesting to note that the rafting forms perpendicular to the maximum principle stress σ_1 in tensile as well as double shear creep tests. It can also be seen from figure 10, the channel width increases with exposure time. After subtracting effects due to the change of morphology associated with rafting, the increase of the mean value of γ -channel width is governed by a parabolic rate law and there is no significant difference between γ -channel widening in a $\langle 001 \rangle$ tension and $\{011\}\langle 01-1 \rangle$ shear creep testing, as shown in figure 11. This suggests that for $\{011\}\langle 01-1 \rangle$ shear loading, the maximum principal stress perpendicular to the γ/γ' -interfaces is important in controlling channel widening kinetics; the additional σ_3 -component in shear testing (as compared to uniaxial tension) has no effect. More work is required to find out whether this conclusion holds for other conditions of multiaxial loading.

6. Practical consequences and suggestions for future work

A wide range of nickel-base single crystal superalloys are developed to improve the efficiency, reliability and operating life of the critical components. The integrity and durability of SX alloys are strongly controlled by the chemical composition and microstructure. It is generally recognised that the change in morphology of phases during creep is due to cross diffusion of alloying elements. Table 2 shows various uniaxial creep testing conditions for the development of rafting in recently developed single crystal superalloys. It is interesting to note that the SX components can be used upto maximum service temperature of 900° C without the effect of rafting. Since the state of stress plays a significant role in the direction of raft development, it is possible to determine the condition of loading

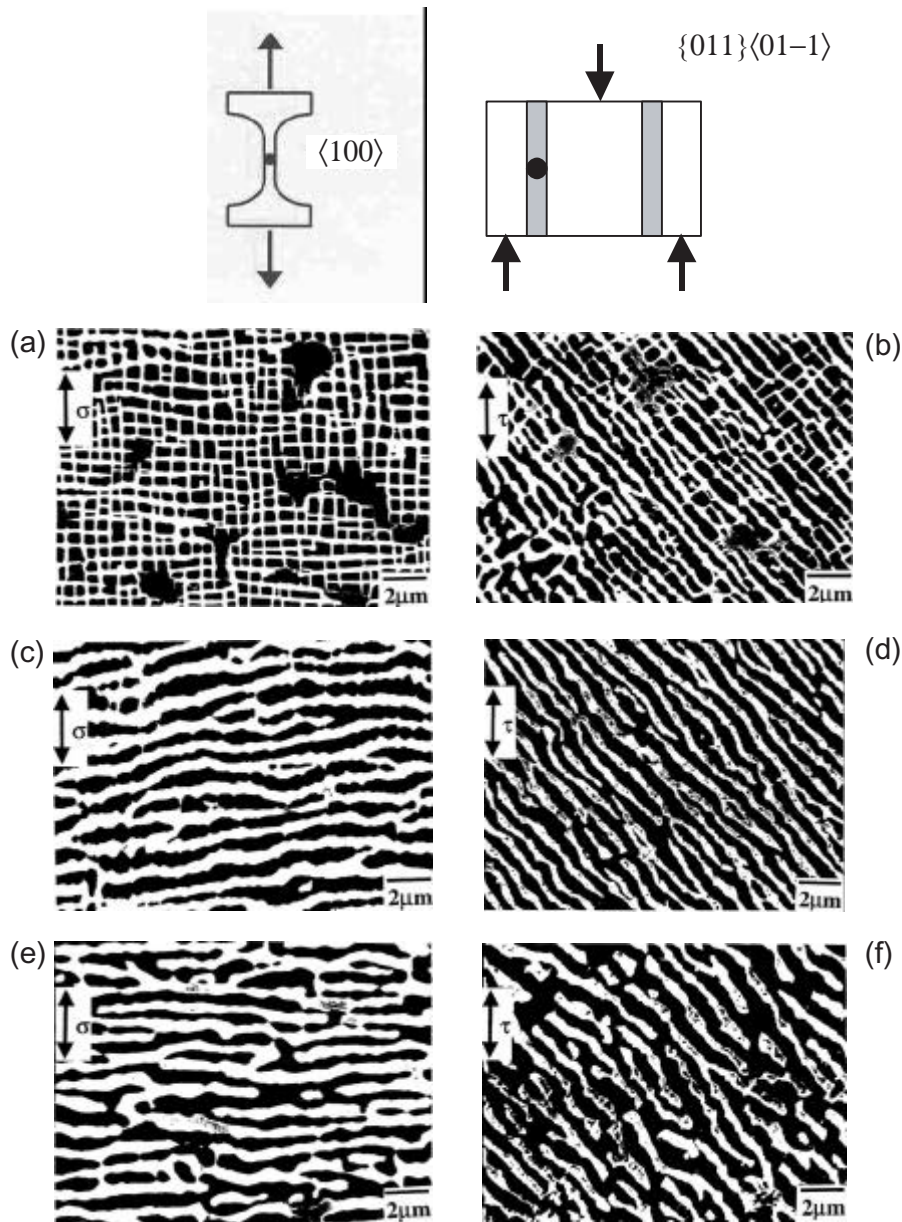


Figure 10. Scanning electron micrographs revealing changes of γ/γ' -phases in CMSX-4 after creep tests at 1080°C and $\sigma_1 = 50\text{MPa}$. Solid marks on specimens show the location of SEM examination: top down view. (a) $\langle 001 \rangle$: 9.9 h; (b) MCSS $\{011\}\langle 01-1 \rangle$: 11.2 h; (c) $\langle 001 \rangle$: 94.8 h; (d) MCSS $\{011\}\langle 01-1 \rangle$: 98.2 h; (e) $\langle 001 \rangle$: 302.4 h; (f) MCSS $\{011\}\langle 01-1 \rangle$: 290.2 h.

during service in case of failure. Thus rafting – its development and growth – can be an effective tool in failure analysis of single crystal components operating at elevated temperature. Since rafting width and size depend on time of load applied at elevated temperature, they can also be used to assess the remaining life of the component with the help of *in situ*

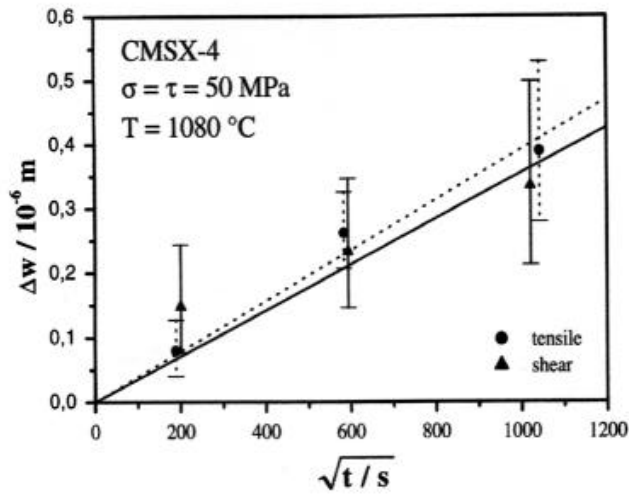


Figure 11. Change of channel widths with time under uniaxial and shear creep test conditions (Kamaraj *et al* 2001).

metallography/non-destructive method. However, the above requires wide experimental data before quantitatively evaluating a procedure for practical applications of a given single crystal superalloy.

Table 2. Rafting in the recent single crystal superalloys.

Material	Test temp. (°C)	Stress (MPa)	Rafting		Stress state: tensile (T)/compression (C) creep	Reference
			Yes	No		
CMSX-4	750	725	×	✓	T	Henderson <i>et al</i> (1999)
	950	155	✓	×	T	Henderson <i>et al</i> (1999)
CMSX-4	950	250	✓	×	T & C	Royer <i>et al</i> (1995)
AM1	1050	140	✓	×	T	Lukäs <i>et al</i> (1996)
CMSX-4	800	767	×	✓	T	Mugharabi <i>et al</i> (1994)
	950	301	✓	×	T	
	1100	80–301	✓	×	T	
SC-83	900	600	✓	×	T	Svetlov <i>et al</i> (1992)
CMSX-3	850	130	×	✓	T	Pollock & Argon (1994)
	850	552	~	~	T	
	900	110	×	✓	T	
	950	95	×	✓	T	
	1050	50	✓	×	T	
	1060	138	✓	×	T	
SRR 99	980	170	✓	×	T	Feller-Kniepmeier (1989)
NASAIR100	760	600–690	×	✓	T	Nathal <i>et al</i> (1989)
NASAIR100	1000	207	✓	×	T & C	Nathal <i>et al</i> (1987)

The author started his work on single crystal nickel base superalloys at the Ruhr-Universität Bochum, Germany. He appreciates collaboration with Prof G Eggeler, Dr M Kolbe, Dr K Neuking and K Serin. The author wishes to acknowledge financial support from the Deutsche Forschungs-Gemeinschaft (Ko 1508/2-3) and from the European Community (Brite-Euram BRPR-CT96-0224). The author is also grateful to Prof V M Radhakrishnan for useful discussions.

References*

- Biermann H, Tetzlaff U, Von Grossmann B, Mughrabi H 2000 *Scr. Mater.* 43: 807–812
- Broomfield R W, Ford D A, Bhangu J K, Thomas M C, Frasier D J, Burkholder P S, Harris K, Erickson G L, Wahl J B 1998 *J. Eng. Gas Turbines Power* 120: 595–608
- Caron P, Khan T 1983 *Mater. Sci. Eng.* 61: 173–184
- Carry C, Strudel J L 1978 *Acta Metall.* 26: 859–870
- Chang J C, Allen S M 1991 *J. Mater. Res.* 6: 1843–1855
- Chen W, Immarrigeon J-P 1998 *Scr. Mater.* 39: 167–174
- Dlouhy A, Eggeler G 1996 *Prakt. Metallogr.* 33: 629
- Dlouhy A, Mayr C, Eggeler G 1997 *Proc. 7th Int. Conf. on Creep and Fracture of Engineering Materials and Science* (eds) J Earthman, F A Mohamed (Warrendale, PA: Minerals Met. Mater. Soc.) p. 677
- Eggeler G, Dlouhy A 1997 *Acta Metall. Mater.* 45: 4251–4262
- Fährmann M, Fährmann E, Paris O, Fratzl P, Pollock T M 1996 In *Superalloys* (eds) R D Kissinger *et al* (Warrendale, PA: Minerals, Met. Mater. Soc.) pp 191–200
- Feller-Kniepmeier M, Link T 1989 *Metall. Trans.* A20: 1233–1238
- Henderson P J, Mclean M 1983 *Acta Metall.* 31: 1203–1219
- Henderson P, Berglin L, Jansson C 1999 *Scr. Metall. Mater.* 40: 229–234
- Ignat M, Buffiere J-Y, Chaix J M 1993 *Acta Metall. Mater.* 41: 855–862
- Kamaraj M, Serin K, Kolbe M, Eggeler G 2000 *Proc. 12th Int. conf. on the strength of materials (ICSMA-12)*, Asilomar, California, USA
- Kamaraj M, Mayr C, Kolbe M, Eggeler G 1998 *Scr. Metall. Mater.* 38: 589–594
- Kolbe M, Dlouhy A, Eggeler G 1998 *Mater. Sci. Eng.* A246 :133
- Kolbe M, Kamaraj M, Heitkemper M, Probst-Hein M, Neuking K, Eggeler G 1988 *Berichtsband der DFG zum Schwerpunktprogramm* (Weinheim: Wiley-VCH) pp 384–396
- Kondo Y, Kitazaki N, Namekata J, Ohi N, Hattori H 1996 In *Superalloys 1996* (eds) R D Kissinger *et al* (Warrendale, PA: Minerals, Met. Mater. Soc.) pp 297–304
- Laberge C A, Fratzl P, Lebowitz J L 1997 *Acta Mater.* 45: 3949–3962
- Leverant G R, Kear B H 1970 *Metall. Trans.* 1: 491–499
- Lukas P, Cadek J, Sustek V, Kunz L 1996 *Mater. Sci. Eng.* A208: 149–157
- MacKay R A, Ebert L J 1983 *Scr. Metall.* 17: 1217–1222
- MacKay R A, Maier R D 1982 *Metall. Trans.* A13: 1747
- Matan N, Cox D C, Rae M F, Reed R C 1999 *Acta Mater.* 47: 2031–2045
- Mayr C, Eggeler G, Dlouhy A 1996 *Mater. Sci. Eng.* A207: 51–63
- Mayr C, 1994 Ph D thesis, Swiss Federal Institute of Technology, Lausanne, Switzerland
- Mayr C, Eggeler G, Webster G A, Peter G 1995 *Mater. Sci. Eng.* A199: 121–130
- McLean M 1983 *Directionally solidified materials for high temperature service* (London: The Metals Society)
- Meetham G W 1981 *The development of gas turbine materials* (London: Applied Science Publishers)
- Mughrabi H, Schneider W, Sass V, Lang C 1994 *10th Int. Conf. Proc. on Strength of Materials* (ed.) Oikawa (Sedai: Japan Inst. Met.) pp 705–708

*References in this paper are not in journal format

- Mughrabi H, Feng H, Biermann H 1995 *Proc. of the IUTAM Symposium on Micromechanics of Plasticity and damage of Multiphase Materials*, France
- Mughrabi H 1996 In *Proc. Johannes Weertman Symp. of TMS*, Anaheim, CA (ed.) R J Arsenault
- Mughrabi H, Ott M, Tetzlaff U 1997 *Mater. Sci. Eng.* A234–236: 434–437
- Mukherji D, Gabrisch H, Chen W, Fecht H J, Wahi R P 1997 *Acta Metall. Mater.* 45: 3143–3154
- Nabarro F R N 1996 *Metall. Trans.* A27: 513–529
- Nabarro F R N 1997 *Scr. Metall. Mater.* 37: 497–501
- Nabarro F R N, Cress C M, Kotschy P 1996 *Acta Mater.* 44: 3189–3197
- Nathal M V 1987 *Metall. Trans.* A18: 1961–1970
- Nathal M V, Ebert L J 1985 *Metall. Trans.* A16: 427–439
- Nathal M V, Mackay R A 1987 *Mater. Sci. Eng.* 85: 127–138
- Nathal M V, Mackay R A, Miner R V 1989 *Metall. Trans* A20: 133–141
- Ohashi T, Hidaka K, Imano S, 1997: *Acta Metall. Mater.* 45: 1801–1810
- Paris O, Fährmann M, Fährmann E, Pollock T M, Fratzl P 1997 *Acta Mater.* 45: 1085–1097
- Pearson D D, Lemkey F D, Kear B H 1980 In *Proc. Fourth Int'l Symp on superalloys* (eds) J K Tien *et al* (Metals Park, OH: ASM) pp 513–519
- Pearson D D, Kear B H, Lemkey F D 1981 In *Creep and fracture of engineering materials and structures* (eds) B Wilshire, D R J Owens (Swansea, UK: Pineridge) p. 213
- Peter G, Probst-Hein M, Kolbe M, Neuking K, Eggeler G 1997 *Mater.-Wiss. Werkstofftech.* 28: 457–464
- Pineau A 1976 *Acta Metall.* 24: 559–564
- Pollock T, Argon A S 1992 *Acta Metall. Mater.* 40: 1–30
- Pollock T M, Argon A S 1994 *Acta Metall. Mater.* 42: 1859–1874
- Royer A, Bastie P, Bellet D 1995 *Philos. Mag.* 72: 669–689
- Sahm P R, Speidel M O 1974 *High temperature materials in gas turbines*, (London: Elsevier Scientific)
- Schneider W, Mughrabi H 1993 *Proc of the 5th Inter Conf on creep and fracture of engineering materials and structures* (eds) B Wilshire, R W Evans (London: Institute of Materials) pp 209–220
- Schneider W, Hammer J, Mugharabi H 1992 In *Superalloys 1992* (eds) S D Antolovich *et al* (Warrendale, PA: Miner., Met. & Mater. Soc.) pp 589–598
- Serin K, Eggeler G 2000b *Prakt. Metallogr.* (to be published)
- Serin K, Neuser R D, Kamaraj M, Kolbe M, Eggeler G, Heitkemper M 2002a *Prakt. Metallogr.* (to be published)
- Shewmon P G 1989 *Diffusion in solids* (Warrendale, PA Miner., Met. & Mater. Soc.)
- Sims C T, Hagel W C 1972 *The Superalloys* (New York: John Wiley & Sons)
- Socrate S, Parks D M 1993 *Acta Metall. Mater.* 41: 2185–2201
- Srinivasan R, Eggeler G, Mills M J 2000 *Acta Mater.* 48: 4867–
- Svetlov I L, Golovko B A, Epishin A I, Abalakin N P 1992 *Scr. Metall.* 26: 1353–1358
- Svoboda J, Lukaš P 1996 *Acta Mater.* 44: 2557–2565
- Swalin R W 1967 *Thermodynamics of solids* (New York: John Wiley & Sons)
- Tian S G, Zhou H H, Zhang J H, Yang H C, Xu Y B, Hu Z Q 2000 *Mater. Sci. Technol.* 16: 451–456
- Tien J K, Copley S M 1971 *Metall. Trans.* A2: 215–219
- Tien J K, Copley S M 1971 *Metall. Trans.* A2: 543–553
- Tien J K, Gamble R P 1972 *Metall. Trans.* A3: 2157–2162
- Véron M, Brechet Y, Louchet F 1996 In *Superalloys* (eds) R D Kissinger *et al* (Warrendale, PA: Miner., Met. & Mater. Soc.), p. 191
- Véron M, Brechet Y, Louchet F 1996 *Acta Metall. Mater.* 45: 3633–3641